Journal of Geriatric Cardiology (2012) 9: 366–374

Research Articles · **Open Access** ·

Hyperpolarization activated cation current (I_f) in cardiac myocytes from pulmonary vein sleeves in the canine with atrial fibrillation

Jia-Yue Li*, Hong-Juan Wang*, Bin Xu*, Xue-Ping Wang, Yi-Cheng Fu, Mei-Yan Chen, De-Xian Zhang, Yan Liu, Qiao Xue, Yang Li

Institute of Geriatric Cardiology, Chinese PLA General Hospital, 28 Fuxing Road, Beijing 100853, China

Abstract

Objective To investigate the characteristics of ectopic automaticity and cation current (I_f) of cardiac myocytes from pulmonary vein sleeves (PVs) in canines with atrial fibrillation. **Methods** The canines (8–10 years old) were subjected to long-term, rapid atrial pacing (RAP) for 10 weeks, which induced the atrial fibrillation model. Disassociation of PVs of canines yielded single cardiac myocytes from a Landengorff column. Action potential, I_f and hyperpolarisation activated cyclic nucleotide-gated (HCN) currents were measured with the patch-clamp technique. **Results** Compared with the control group, cardiac myocytes from the RAP canine PVs had spontaneous diastolic depolarization, shorter action potential duration, and larger I_f densities. In the group of RAP cells, the half maximal activation potential ($V_{1/2}$) was found to be less negative (–105.5 ± 5.2 mV) compared to control cells (–87.3 ± 4.9 mV). Current densities of I_f were increased significantly by β-adrenergic receptor stimulation with isoproterenol and caused an acceleration of current activation. In contrast, I_f currents in the RAP were reduced by carvedilol, a selective beta-adrenergic receptor. Another important finding is that HCN4-based channels may make a significant contribution to I_f in PVs cells, but not HCN2. Meanwhile, HCN4 current significantly increases in canine PVs cardiac myocytes with RAP. **Conclusions** The spontaneous action potential and larger I_f current were observed in the PVs cardiac myocytes using RAP, which may contribute to more ectopic activity events to trigger and maintain atrial fibrillation.

J Geriatr Cardiol 2012; 9: 366–374. doi: 10.3724/SP.J.1263.2012.04161

Keywords: Cation current; Cardiac myocytes; Canine; Atrial fibrillation; β-receptor

1 Introduction

Atrial fibrillation (AF) is the most common sustained tachyarrhythmia and is one of the major causes of stroke.[1,2] The myocardial fibers of the left atrium wrap around the pulmonary vein sleeve (PVs) entering the left atrium to form myocardial sleeves and this structure is the origin of focal electrical activity. Recent clinical trials have shown that paroxysmal AF is initiated by ectopic foci in "sleeves" of atrial tissue within the pulmonary veins or vena caval junctions. Catheter ablation of triggers originating from the PVs may successfully terminate paroxysmal atrial fibrillation. Previous studies showed that there was ectopic rhythm originating from the PVs. An ectopic rhythm originating from the PVs is important not only for the initiation of AF, but also for its maintenance.[3–5]

The cardiac hyperpolarization activated cation current (I_f) is known to be present in regions with primary or secondary pacemaker activity, which is found in non-pacemaking regions of heart. In pacemaking regions, I_f is believed to contribute to spontaneous diastolic depolarization. It was speculated that I_f could elicit abnormal automaticity of cardiac myocytes of PVs and thus, play a role in atrial fibrillation.[6,7] In this study, we investigated the electrophysiological and pharmacological characteristic of I_f in canine cardiac myocardium of PVs with AF by rapid atrial pacing (RAP).

2 Methods

2.1 Preparation of animal model

Twelve dogs (20 ± 3 kg, 8–10 years old) were anesthetized with pentobarbital (30 mg/kg, i.v.). The normal canines (n = 6) served as control group, and the canines subjected to long-term RAP (n = 6) as the RAP model group. Mechanical ventilation was maintained via an endotracheal tube using a mechanical ventilator (Model SN-480-5, Shinano Manufacturing, Tokyo, Japan) with 100% oxygen. Two pa-

***The authors contributed equally to this paper.**

Correspondence to: Yang Li & Qiao Xue, Institute of Geriatric Cardiology of Chinese PLA General Hospital, 28 Fuxing Road, Beijing 100853, China. E-mails: liyangbsh@163.com (Li Y); xueqiao301@sina.com (Xue Q).

Telephone: +86–10-66936762 **Fax:** +86-10-66936782

Received: April 16, 2012 **Revised:** October 31, 2012

Accepted: November 7, 2012 **Published online:** December 10, 2012

irs of stainless steel wire electrodes were sutured against the epicardial surface of the right atrial (RA) free wall within the pectinate muscle area and left atrial appendage. The other ends of the wire electrodes were tunneled subcutaneously and exposed at the back of the neck. For continuous rapid, atrial pacing, a unipolar screw-in pacing lead (CapSureFix 5568, Medtronic Inc., Minneapolis, MN, USA) was inserted through the right external jugular vein, with the distal end of the lead screwed into the endocardial side of the right atrial appendage (RAA). The proximal end of the pacing lead was connected to a rapid pulse generator, which was implanted into a subcutaneous pocket in the neck.[8] The pacing canines received RAP (at a rate of 800 beats/min) for 10 weeks in the conscious and freely moving state. All of these canines developed sustained atrial fibrillation after long-term RAP. To obtain stable baseline conditions, each dog was allowed to recover after the initial surgical procedure for at least one week without pacing. In six dogs, RAP (800 beats/min) was initiated after this recovery period and continued for 10 weeks. Continuous rapid pacing was not performed in the remaining three dogs, which comprised the non-pacing control group, for the evaluation of mRNA expression.

To evaluate AF inducibility, the incidence of AF induction was evaluated with atrial burst pacing for 3 s at the minimal pacing cycle length that achieved 1: 1 atrial capture at each pacing site. This pacing was delivered at 4-fold the diastolic threshold with a pulse width of 2 ms. When AF was induced, its duration was measured. We defined AF as a spontaneous irregular atrial rhythm lasting longer than 1 s. The atrial burst pacing for AF induction was delivered 5 times at each pacing site and at each evaluation time point during the entire protocol.

2.2 Reagents and solutions

(±)-Isoproterenol (Iso, Sigma Co.) was dissolved in distilled water to make a stock solution. Ivabradine (Iva, Institut de Recherches Internationales Servier, France) was added to the extracellular solution by dissolving a stock solution to the final concentration desired. These reagents were diluted to final concentration with extracellular solution in the experiment. Tetrodotoxin, $BaCl_2$, $CdCl_2$ and 4-aminopyridine were from Sigma Co.

Tyrode solution contained (mmol/L): NaCl 136, KCl 5.4, $MgCl_2$ 1, $CaCl_2$ 1, NaH_2PO_4 0.33, 4-(2-Hydroxyethyl)-1-piperazineethanesulfonic acid (HEPES) 5 and dextrose 10 (pH 7.35 with NaOH). Ca^{2+}-free Tyrode's solution, which was omitted Ca^{2+} from Tyrode's.

The pipette solution recording action potentials contained (mmol/L): KCl 120, $MgCl_2$ 1, Na_2ATP 5, HEPES 10, EGTA 0.5 and $CaCl_2$ 0.01, adjusted to pH 7.2 with 1 mol/L KOH. To visually identify whether the cells had pacemaker activity, we did not add ionic current blockers in the pipette solution.

The external solution recording I_f contained (mmol/L): NaCl 137, KCl 25, $CaCl_2$ 1.8, $MgCl_2$ 1.2, $BaCl_2$ 1, $MnCl_2$ 2, $CdCl_2$ 0.2, 4-aminopyridine 3, glucose 5, HEPES 5, adjusted to pH 7.35 with NaOH. To record I_f, sodium current was blocked with 50 μmol/L tetrodotoxin, and inward rectifier potassium current was blocked by Ba^{2+} ($\leq$ 5 mmol/L, to avoid inhibiting I_f with higher concentration of Ba^{2+}).

The pipette solution recording I_f contained (mmol/L): K^+-aspartate 100, KCl 30, Na_2ATP 5, $CaCl_2$ 4, EGTA 11, HEPES 10, adjusted to pH 7.2 with KOH. Ba^{2+}, Cd^{2+} and 4-aminopyridine were added to reduce the interference of potassium and calcium currents.

2.3 Isolation of PVs single cardiac myocytes

The canines were anaesthetized with pentobarital (30 mg/kg, i.v.) and artificially ventilated at room temperature. Hearts and adjacent lung tissue were quickly excised through a left lateral throacotomy and immersed in oxygenated Tyrode's solution at room temperature. To isolate PV cardiac myocytes, the proximal circumflex artery was cannulated. The veins were separated from the lung parenchyma about 20 mm distal to the ending of the myocardial extension onto the PVs. The isolated PVs were ligated with silk thread. The PVs were perfused with oxygenated Tyrode's solution and then replaced with oxygenated Ca^{2+}-free Tyrode's solution containing 300 U/mL collagenase (Type II, Sigma Biochemical St. Louis, MO, USA) and 0.5 U/mL protease (Type IV, Sigma-Aldrich, St. Louis, MO, USA). After a period of 40–45 min, PVs were well-perfusing and single cardiac myocytes could be isolated from all veins.[9] The solution was gradually changed to normal oxygenated Tyrode solution. Only cells showing rob-shape and quiescent cells were used (Figure 1). Experiments were carried out at temperature of 36 ± 0.5°C.

2.4 Transfection of HEK 293 cells

HEK 293 cells (ATTC, Manassas, VA, USA) were maintained under 5% CO_2 in humidified air at 37℃ as indicated for biochemical analysis. The RNA was isolated from cardiac muscle tissue samples from PVs of Control and RAP using a commercial RNA extraction kit (RNAiso Plus, TAKARA, China) and cDNA synthesized with Primescript RT reagent Kit (TAKARA, China) in accordance with the instructions of the manufacturer (Forward and Reverse primer, see section 1.5). And then, hyperpolarisation activated cyclic nucleotide-gated (HCN)2 and HCN4 channels cDNA were, respectively, combined with vehicle plasmid of pcDNA3.1. Cell pellets were plated on laminin-coated 35 mm

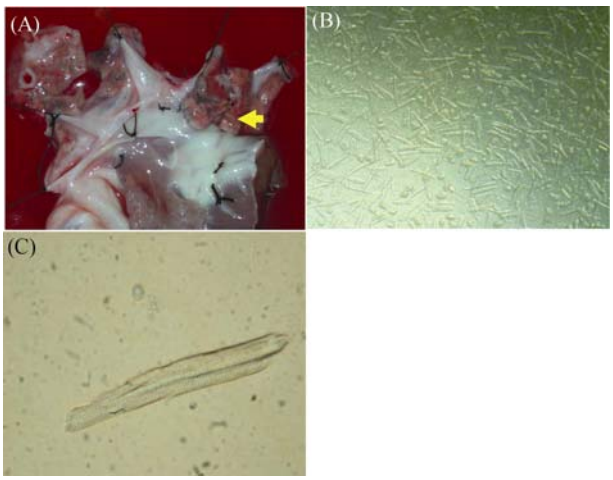

Figure 1. Cardiac myocytes and tissue from pulmonary vein sleeves in canine. (A): PVs tissue (yellow arrow); (B): PVs myocytes (100 ×); (C): PVs myocytes (400 ×). PVs: pulmonary vein sleeves.

dishes. Transient transfection of HCN2 and HCN4 channel cDNA plasmid pcDNA3.1 2.0 μg and 5 μL lipofectamine transfection reagents were performed into the cultured cells by using Lipofectamine (Life Technologies, Gaithersrburg, MD, USA) following the manufacturer's instructions. CD8 cDNA was co-transfected as a reporter gene (EBo-pCD vector, American Type Culture Collection). CD8-positive cells were identified using Dynabeads (Dynal, M-450 CD8). Cells were harvested at 48–72 h after transfection. 25% to 30% of transfection positives rate were identified. The recording strategy and condition of HCN2 and HCN4 currents were similar to those of the isolated PVs cardiacmyocytes.

2.5 Reverse transcription-polymerase chain reaction (RT-PCR)

The RNA was isolated from 50 mg to 100 mg frozen cardiac muscle tissue samples from PVs of Control and RAP using a commercial RNA extraction kit (RNAiso Plus, TAKARA, China) and cDNA synthesized with Primescript RT reagent Kit (TAKARA, China; reaction condition: 37°C, 15 min; 85°C, 5 s) in accordance with the instructions of the manufacturer. HCN2: Forward primer: 5′-CCATGCTGACA AAGCTCAAA-3′, Reverse primer: 3′-CGAGCTGAGAT CATGCTGAA-5′; HCN4: Forward primer: 5′-GGGCTT CTCCTGTAGCCTTT-3′, Reverse primer: 3′-TGAGCTT CAGGTCCTGTGTG-5′. The cDNA generated was amplified using specific primers designed for HCN2, HCN4 and glyceraldehyde phosphate dehydrogenase (GAPDH). The nucleotide sequences and Tm value of all primers given in PCR products were visualized under UV light with Ethidium-Bromide (Sigma) staining in 2.0% agarose gels. Images were captured with GelDoc XR (BioRad, America), and then the band intensity was determined with Quantity One software.

2.6 Electrophysiological recording

Currents were recorded with the whole-cell, patch-clamp technique by means of an Axon-700B amplifier (Axon Instruments, Inc., Foster City, CA, USA) at 36 ± 0.5°C. Current signals were filtered at 3 kHz, through a 16-bit A/D digital converter (Digidata 1322A, sampling rate 1.0 kHz; Axon Instruments, Inc.). Borosilicate glass electrodes were used, with tip resistances of 3 to 5 MΩ. Junction potentials averaged 5.0 ± 0.5 mV was corrected prior to formation of gigahom seals. 87% of the series resistance and capacitive time constant (τ) were compensated. Capacitance was assessed using 5 mV, 5 ms hyperpolarizing steps from a holding potential of -70 mV. The action potentials were recorded in current-clamp mode and ionic currents in voltage-clamp mode. Original recordings are shown in terms of current amplitude, but mean data are presented as current density (pA/pF) for variability in cell size (cell membrane capacitance). Trace acquisition and analysis was controlled by dedicated software (pClamp 9.2; Axon Instruments, Inc.)

2.7 Data analysis and statistical methods

Off-line leak correction was performed on all amplitude data. Data were presented as mean ± SE, with *n* representing the number of cells analyzed. pCLAMP version 9.2 (Axon Instruments) and Origin (Microcal Software) software were used for data analysis. Statistical significance was evaluated using Student's *t*-test, one way ANOVA and repeated-measures ANOVA. Percent was evaluated using a fish analysis method. A value of $P < 0.05$ was defined as statistically significance.

3 Results

3.1 Successful rates of modeling and mortality of animals

One of six sham canines was AF (16.7 %), and in five canines operated with RAP, there were four modeled successfully (80.0 %, $P < 0.01$). In RAP group; there was one with pneumatothorax dead at the 4th day after operation.

3.2 Action potential configurations of PV cardiac myocytes

The spontaneous action potentials in some PVs cells were recorded directly, while action potentials in other cells were induced by using test current pulse of 900 pA for 5 ms from a holding potential of 0 mV. The results showed that there were more events of spontaneous diastolic depolarization in cardiac myocytes of PVs with RAP, with an AP of

the PVs cardiac myocytes without pacemaker activity (12/20, 60.0%) and a spontaneous AP with RAP (19/23, 82.6%). The maximum diastolic potentials (–63 ± 2 mV *vs.* –65 ± 3 mV) showed no significant difference between the RAP and control groups. The action potential amplitude (83 ± 3 mV) in RAP canine PVs cells was smaller than that of the control (90 ± 2 mV). The APD_{50} in RAP canine PVs cells (107 ± 9 ms) was significantly shorter than that of control canines (129 ± 12 ms), while APD_{90} in RAP canine PVs cells was prolonged (from 282 ± 11 ms to 343 ± 14 ms, $P < 0.05$, Figure 2).

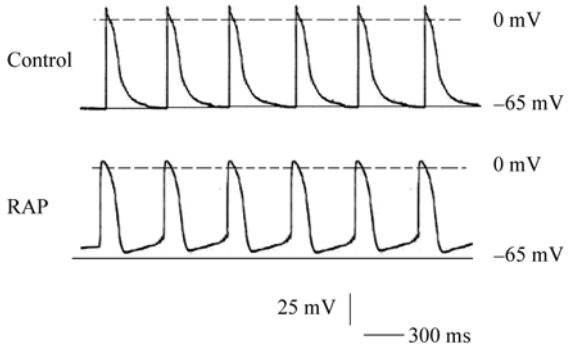

Figure 2. APs configurations of PV cardiac myocytes with and without rapidly atrial pacemaking. (A): APs of control cells with rest potential of –65 ± 3 mV and APD_{90} of 282 ± 11 ms; (B): Spontaneous AP of PVs cells with maximum diastolic potentials of –63 ± 2 mV and APD_{90} of 343 ± 14 ms. The spontaneous APs in some PVs cells were recorded directly, while APs in other cells were induced by using test current pulse of 900 pA for 5 ms at a holding potential of 0 mV. APs: action potentilas; PVs: pulmonary vein sleeves; RAP: rapid atrial pacing.

3.3 Characteristics of I_f current of PV cardiac myocytes

The presence of I_f was determined in cells by application of hyperpolarizing voltage steps in 10 mV increments from –50 mV to –120 mV for 2000 ms duration form a holding potential of –40 mV, and then depolarized to +20 mV for 200 ms to elicit tail current. Current traces obtained in representative cells from Control and RAP are recorded (Figure 3A). I_f current densities were significantly higher in RAP than in control cells at potentials –120 mV (–2.66 ± 0.41 pA/pF *vs.* –0.91 ± 0.22 pA/pF, $P < 0.01$, $n = 10$, Figure 3B). In both groups of cells, the voltage clamp protocol elicited a time-dependent inward current that increased in amplitude and activated more rapidly with progressively more negative test potentials. Figure 3C illustrates the mean I_f current-voltage relationship curve. Activation procedure of I_f in the RAP myocytes was well fitted by a mono-exponential equation at potentials positive to –90 mV, with averaged activation time-constant (τ) of 102 ± 13 ms. In most cases a bi-exponential fit was more accurate in describing the I_f time course at more negative test potentials (lower –90 mV), with an averaged fast activation time-constant ($\tau 1$) of 76 ± 8 ms and an averaged slow activation time-constant ($\tau 2$) of 2366 ± 217 ms. In contrast, this procedure of I_f in the control myocytes was well fitted by a mono-exponential equation at any test potential, with an averaged activation time-constant (τ) of 1725 ± 24 ms. In addition, the voltage dependence of activation was determined from tail currents at –40 mV following 4000 ms test pulses; interpulse intervals were 15 s to ensure complete deactivation of I_f channels. The steady-state activation curve of I_f were elicited by 10 mV steps hyperpolarized from –50 mV to –150 mV for 2000 ms, following +20 mV 200 ms for tail current. The variable of voltage-dependent activation of tail current was calculated by basing on the formulation $G = I/(V_t–V_r)$ as described previously, where G means the peak conductance at the test voltage (V_t), and V_r means the measured reversal potential. Mean data for activation, along with best-fit Boltzmann equation, was utilized to obtain the half activation voltage ($V_{1/2}$) and the slope (k); $G/G_{max}=1/\{1 + \exp[(V_t–V_{1/2})/k]\}$. In the steady-state activation curve, $V_{1/2}$ was changed from –105.5 ± 5.2 mV in control cells to –87.3 ± 4.9 mV in the RAP group and k was changed from 9.5 ± 1.8 mV to 11.1 ± 2.6 mV (Figure 3D).

3.4 Effect of isoprenaline on I_f of PV cardiac myocytes

The result showed that I_f was markedly increased by the application of 1.0 μmol/L isoprenaline (Figure 4A). At –120 mV of test potential, peak currents of I_f of RAP cells were increased from –2.66 ± 0.41 pA/pF to –3.47 ± 0.73 pA/pF by 1.0 μmol/L Iso ($P < 0.01$, $n = 11$), while peak currents of I_f of RAP cells were increased from –0.91 ± 0.22 pA/pF to –1.32 ± 0.13 pA/pF by 1.0 μmol/L isoprenaline ($P < 0.01$, $n = 11$). Isoprenaline-induced effects on I_f of RAP were tested under the concentration of 0.1, 0.3, 1.0, 3.0 and 10.0 μmol/L and the EC_{50} value was 0.7 μmol/L (0.4–1.5 μmol/L, 95% CI; Figure 4C) by the Marquardt-Levenberg formulation. I-V relationships demonstrated I_f densities were markedly enhanced by 1.0 μmol/L isoprenaline more negative –80 mV potentials with a repeated-measures ANOVA. It showed the voltage dependence of I_f activation was significantly affected by the application of isoprenaline. The inward current increased in amplitude and activated more rapidly by isoprenaline with progressively more negative test potentials (Figure 4D). Effect of isoprenaline on steady-state activation curve of I_f showed that $V_{1/2}$ of activation was shifted from –87.3 ± 4.9 mV to 69.3 ± 3.4 mV and k value was changed from 9.5 ± 1.8 mV to 8.7 ± 1.2 mV by 1.0 μmol/L isoprenaline ($P < 0.01$, $n = 14$, Figure 4E). Responses with isoprenaline, more events of spontaneous diastolic depolarization in PVs cardiac myocytes, were observed (Figure 4F).

3.5 Effect of ivabradine on I_f of PV cardiomyocytes

To investigate the pharmacologic characteristics of I_f channel of PVs cells, I_f was substantially inhibited by the application

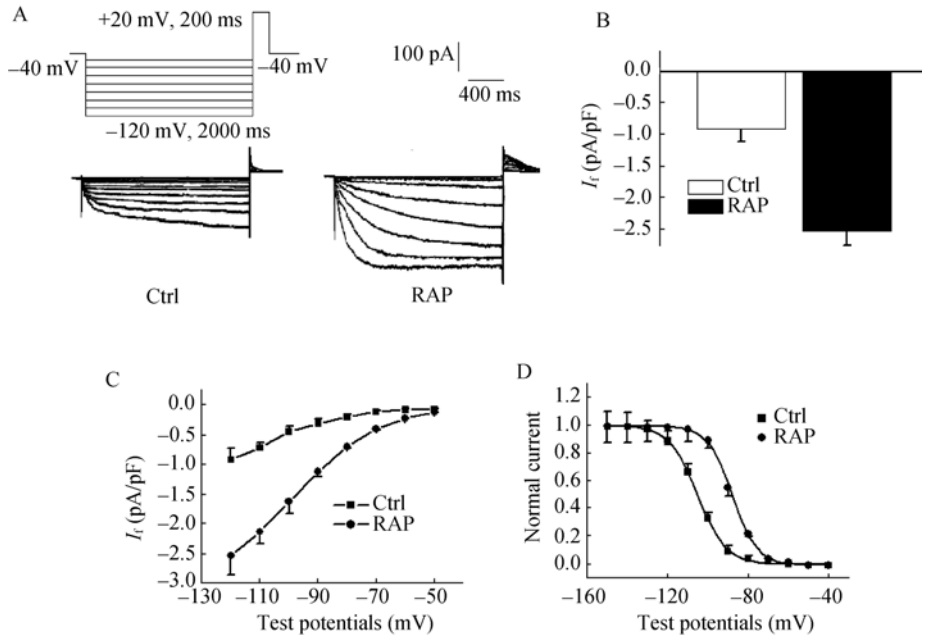

Figure 3. I_f current characteristics of PVs cardiac myocytes. (A): I_f current densities were significantly higher in RAP than in control cells at potentials −120 Mv; (B): RAP: −2.66 ± 0.4 pA/pF *vs*. Ctrl: −0.91 ± 0.2 pA/pF, $P < 0.01$, $n = 10$; (C): the current–voltage relationships of the mean I_f for RAP and control cells; (D) the steady-state activation curve showed that $V_{1/2}$ was changed from −105.5 ± 5.2 mV in control cells to −87.3 ± 4.9 mV in RAP group and k was changed from 9.5 ± 1.8 mV to 11.1 ± 2.6 mV. The presence of I_f was determined in cells by application of hyperpolarizing voltage steps from −50 to −120 mV in 10 mV increments of 2000 ms duration at the holding potential of −40 mV, and then depolarized to +20 mV for 200 ms to elicit tail current. Current traces obtained in representative cells from Control and RAP. PVs: pulmonary vein sleeves; RAP: rapid atrial pacing.

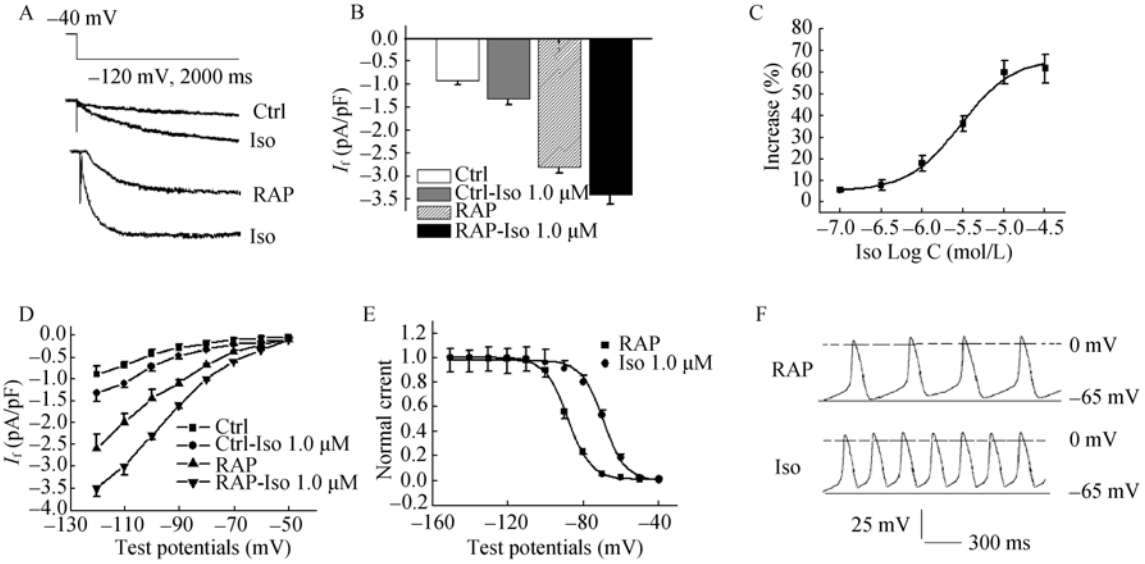

Figure 4. Effect of Iso on I_f of PVs cardiac myocytes. Peak current of I_f was increased from −2.66 ± 0.4 pA/pF to −3.27 ± 0.7 pA/pF to −3.47 ± 0.73 pA/pF by 1.0 μmol/L Iso ($P < 0.01$, $n = 11$), while peak currents of I_f of RAP cells were increased from −0.91 ± 0.22 pA/pF to −1.32 ± 0.13 pA/pF by 1.0 μmol/L Iso at −120 mV of test potential ($P < 0.01$, $n = 11$, A & B); (C): Iso-induced increase of I_f was tested under the concentration of 0.1–10.0 μmol/L and the EC_{50} value was 0.7 μmol/L (0.4–1.5 μmol/L, 95% CL); (D): I-V relationships demonstrated I_f densities were markedly enhanced by 1.0 μmol/L Iso more negative −80 mV potentials with a repeated-measures ANOVA. It showed the voltage dependence of I_f activation was significantly affected by the application of Iso; (E): $V_{1/2}$ for activation was shifted from −88.3 ± 4.7 mV to 69.3 ± 3.4 mV and k value was changed from 9.5 ± 1.8 mV to 5.2 ± 1.2 mV by 1.0 μmol/L Iso ($P < 0.01$, n =11); (F): More events of spontaneous diastolic depolarization in PVs cardiac myocytes with Iso were observed. EC_{50}: concentration for 50% of maximal effect; Iso: isoprenaline; PVs: pulmonary vein sleeves; RAP: rapid atrial pacing.

of ivabradine (Figure 5A). At -120 mV of test potential, peak current densities of I_f in RAP cells was reduced from –2.74 ± 0.52 pA/pF to –1.47 ± 0.26 pA/pF ($P < 0.01$, n =12), while densities of I_f in control cells was reduced from –0.93 ± 0.20 pA/pF to –0.61 ± 0.05 pA/pF by 1.0 μmol/L ivabradine. Both inhibition effects showed significant difference (inhibition percent of 46.4% in RAP cells *vs*. 33.3% in control cells, $P < 0.05$). I-V relationships demonstrated that inhibition of 1.0 μmol/L Iva on I_f density more negative –90 mV potentials with a repeated-measures ANOVA (Figure 5B). Concentration dependences of ivabradine-induced inhibition on I_f from two groups were tested with the concentration of 0.1, 0.3, 1.0, 3.0 and 10.0 μmol/L and the IC_{50} value were 3.2 μmol/L by the Marquardt-Levenberg formulation $I = I_{max}/(IC_{50}/[C]+1)$ (Figure 5C). The spontaneous AP events were reduced by 1.0 μmol/L Iva (Figure 5D).

3.6 mRNA expression and current characteristics of HCN2 and HCN4 in PVs of control and RAP

Figures 6A and 6B showed that HCN2 mRNA expression levels were not statistically significantly different between both the control and RAP groups. HCN4 mRNA level was much higher than that in the control group. At test potential of –120 mV, HCN4 current from PVs in RAP model significantly increased (Ctrl: 1.81 ± 0.3 pA/pF *vs*. RAP: 3.34 ± 0.7 pA/pF, $P < 0.05$, $n = 15$) ,while HCN2 current from PVs in the RAP model change was not observed (Ctrl: 0.38 ± 0.04 pA/pF *vs*. RAP: 0.46 ± 0.05 pA/pF, $P > 0.05$, Figure 6C–E). I-V relationship curves showed that HCN4 current densities were significantly higher in RAP than in control cells, range of –80 and –120 mV. Furthermore, with test potentials shifting to a negative direction, acceleration of HCN4 current was observed. At all test potentials, HCN2 current densities of control were markedly lower than that of HCN4. In the RAP model, HCN2 slightly increased but was not statistically significance (Figure 6F).

4 Discussion

Clinical electrophysiology studies in patients have demonstrated that rapid focal activity originating from PV can trigger and maintain atrial fibrillation.[8–10] The major finding of the present study is that the pacing-induced spontaneous action potential and larger I_f current were observed in the PVs cardiac myocytes from canine using RAP. Although the maximum diastolic potential of PVs cells from RAP

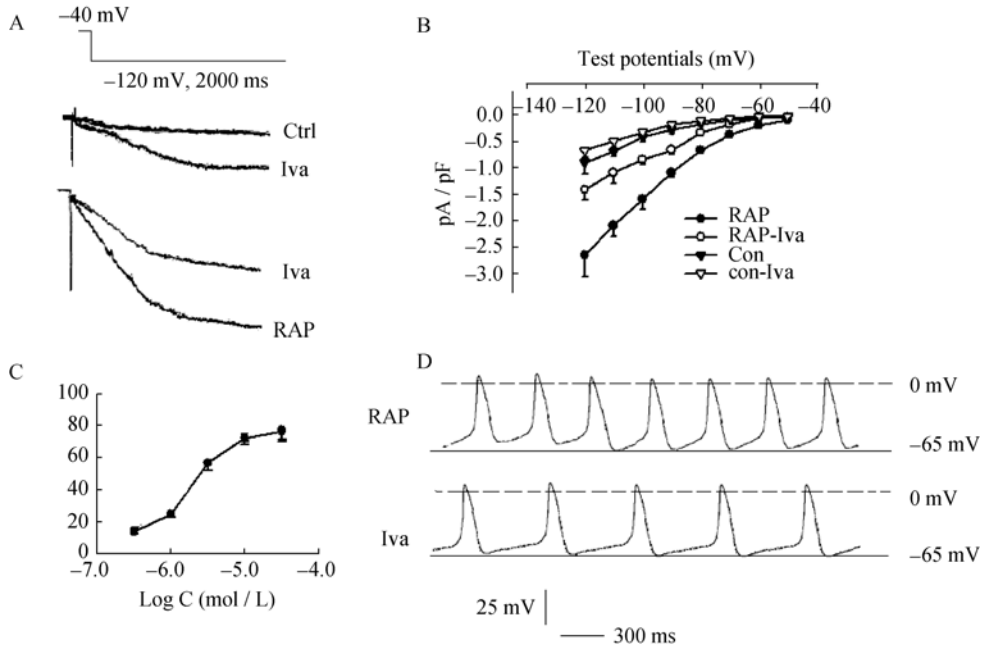

Figure 5. Effect of Ivabradine on I_f of PVs cardiomyocytes. (A): peak current densities of I_f in RAP cells were reduced from –2.74 ± 0.52 pA/pF to -1.47 ± 0.26 pA/pF ($P < 0.01$, n = 12), while densities of I_f in control cells were reduced from –0.93 ± 0.20 pA/pF to –0.61 ± 0.05 pA/pF by 1.0 μmol/L Iva. Both inhibition effects showed significant difference (inhibition percent of 46.4% in RAP cells *vs*. 33.3% in control cells, $P < 0.05$); (B): I-V relationships demonstrated that significantly inhibited effects of 1.0 μmol/L Iva on I_f density more negative –90 mV potentials with a repeated-measures ANOVA; (C) Iva-induced inhibition concentration dependence of I_f was tested under the concentration of 0.1–10.0 μmol/L and the IC_{50} value was 3.2 μmol/L in RAP and control cells respectively; (D): The events of spontaneous diastolic depolarization were reduced by 1.0 μmol/L Iva. Iva: ivabradine; PVs: pulmonary vein sleeves; RAP: rapid atrial pacing.

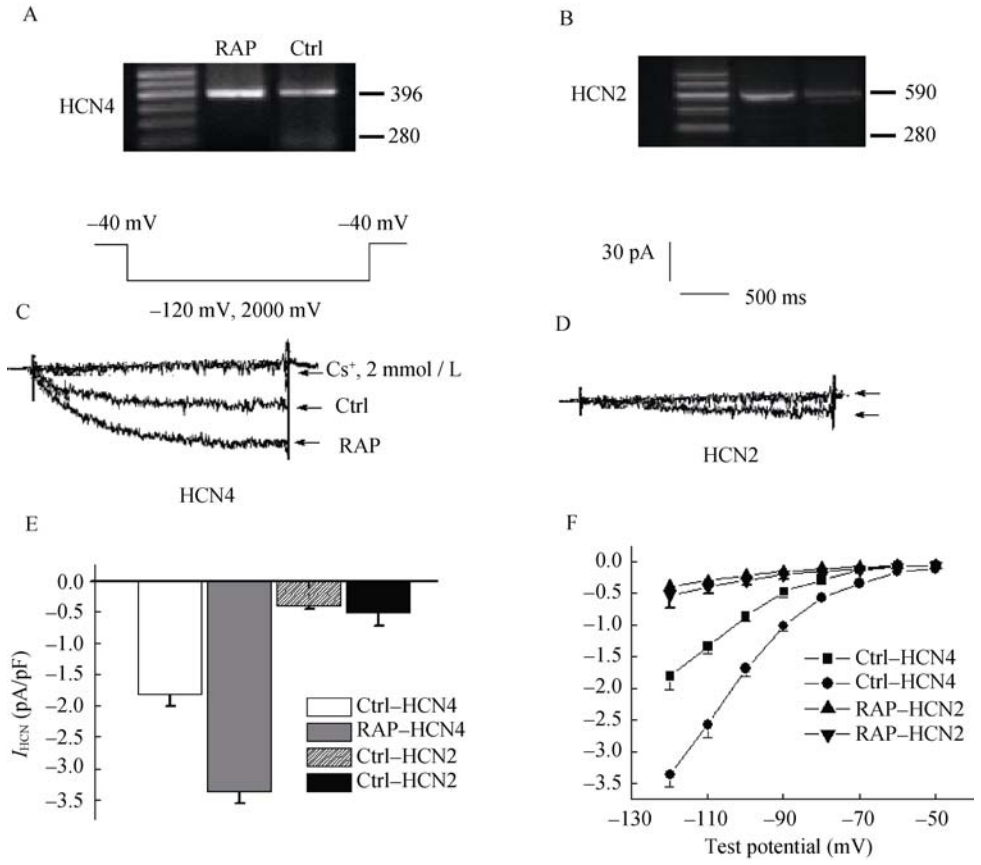

Figure 6. mRNA expression of HCN4 and HCN2 from PVs myocytes and current characteristics with HEK cells. (A) & (B) showed that HCN2 and HCN4 mRNA expression levels of control and RAP groups. Current traces of HCN4 and HCN2 from Control and RAP PVs cells was showed in (C) and (D); (E): peak current densities of HCN4 and HCN2 from PVs in RAP model at test potential of –120 mV; (F): I-V relationship curve showed that HCN4 current densities were significantly higher in RAP than in control cells range of –80 and -120 mV, but not HCN2. HCN: hyperpolarisation activated cyclic nucleotide-gated channels PVs: pulmonary vein sleeves; RAP: rapid atrial pacing.

was close to those of control group, a slow diastolic depolarization in the PVs cells was found. This spontaneous depolarization event would drive the membrane voltage above the threshold level and generated action potential. The action potential from PVs, as an initiation of ectopic activity, may play a role in the occurrence of atrial fibrillation arose from these cells.[11–13]

To investigate the mechanism of spontaneous action potential from PVs, we study the I_f densities, activation kinetics and activation duration of the cardiac myocytes isolated from the PVs. I_f current densities were significantly higher than those in control cells at the test potentials. Original I_f showed the most positive $V_{1/2}$ value in RAP cells at hyperpolarized membrane potentials (with faster activation at more negative potentials).

The sensitivity to β-adrenergic stimulation may be a strong evidence for the adrenergic type of paroxysmal atrial fibrillation, which occurs under the states of increased adrenergic activity and spontaneously terminate accompanied by a reduction of the elevated sympathetic tone. Lee, *et al*.[14] showed that ventricular and dual chamber pacing increases tissue catecholamine activity in dogs. Similarly, Fukuoka, *et al*.[15] reported that long-term ventricular pacing in humans, even in the presence of atrioventricular synchrony, accelerates cardiac sympathetic activity. β-adrenergic stimulation, by increasing the intracellular concentration of cAMP in pacemaker cells, increases the I_f current and the slope of the diastolic depolarization, which decreases the diastolic time and accelerates the heart rate.[16,17] We found that β-adrenergic receptor stimulation with isoprenaline could significantly increase I_f current densities and cause an acceleration of current activation with a $V_{1/2}$ shift to more positive potential. It was suggested that isoprenaline may significantly increase I_f of pulmonary veins sleeves cells with atrial fibrillation caused by RAP. Furthermore, more events of spontaneous diastolic depolarization in PVs cardiac myocytes after with treatment of isoprenaline were observed. We presumed that ectopic activity events of PVs cells of canine are easier development

as these cells possessed larger I_f current densities. To confirm this hypothesis, we investigated effect of Iva, a selected blocker of I_f current,[18,19] on PVs cells of the canine. It was found that Iva markedly reduced I_f currents in the RAP cells in a concentration-dependence manner. The direct electrophysiological consequence of Iva blockade of I_f is a reduction in the slope of the diastolic depolarization, leading to an increase in the time interval between successive action potentials and consequently a decrease in heart rate. Our results suggested that ivabradine might be a therapeutic agent of AF due to inhibition of the pacemaking current in PVs cells.

Structural subunits of native f-channels are the HCN channels. HCN channels comprise a small subfamily of proteins within the super family of pore-loop cation channels. HCN channels are encoded by four genes (HCN1–4) and are widely expressed throughout the heart and the central nervous system. HCN2 and HCN4 channels seem to play the predominant role in cardiac pacemaker tissue. HCN4 is most highly expressed in SAN tissue.[20–22] Another important finding is that HCN4-based channels may make a significant contribution to I_f in PVs cells, but not HCN2. Meanwhile, HCN4 current significantly increases in canine PVs cardiac myocytes with RAP. It suggested that HCN4 current may contribute partly to ectopic activity in the occurrence of atrial fibrillation.

The spontaneous action potential and larger I_f current observed in the PVs cardiac myocytes using RAP contribute to more ectopic activity events to trigger and maintain atrial fibrillation. These observations provide new insights into the potential mechanisms behind the increased prevalence of AF with RAP.

Acknowledgements

This study was supported by the National Natural Science Foundation of China (No: 81170177, No: 30770901).

References

1 Brundel BJ, Shiroshita-Takeshita A, Qi X, *et al*. Induction of heat shock response protects the heart against atrial fibrillation. *Circ Res* 2006; 99:1394–402.

2 Miyazaki S, Kuwahara T, Kobori A, *et al*. Prevalence, electrophysiological properties, and clinical implications of dissociated pulmonary vein activity following pulmonary vein antrum isolation. *Am J Cardiol* 2011; 108: 1147–1154.

3 Wang TM, Chiang CE, Sheu JR, *et al*. Homogenous distribution of fast response action potentials in canine pulmonary vein sleeves: a contradictory report. *Int J Cardiol* 2003; 89: 187–195.

4 Gao CH, Wang F, Jiang R, *et al*. A region-specific quantitative profile of autonomic innervation of the canine left atrium and pulmonary veins. *Auton Neurosci* 2011; 162: 42–47.

5 Honjo H, Boyett MR, Niwa R, *et al*. Pacing-induced spontaneous activity in myocardial sleeves of pulmonary veins after treatment with ryanodine. *Circulation* 2003; 107: 1937–1943.

6 Hamabe A, Okuyama Y, Miyauchi Y, *et al*. Correlation between anatomy and electrical activation in canine pulmonary veins. *Circulation* 2003; 107: 1550–1555.

7 Bois P, Guinamard R, Chemaly AE, *et al*. Molecular regulation and pharmacology of pacemaker channels. *Curr Pharm Des* 2007; 13: 2338–2349.

8 Von Bary C, Weber S, Dornia C, *et al*. Evaluation of pulmonary vein stenosis after pulmonary vein isolation using a novel circular mapping and ablation catheter (PVAC). *Circ Arrhythm Electrophysiol* 2011; 4: 630-636.

9 Ehrlich JR., Tae-Joon C, Liming Z, *et al*. Cellular electrophysiology of canine pulmonary vein cardiomyocytes: action potential and ionic current properties. *J Physiol* 2003; 551: 801–813.

10 Chen YJ, Chen SA, Chang MS, *et al*. Arrhythmogenic activity of cardiac muscle in pulmonary veins of the dog: implication for the genesis of atrial fibrillation. *Cardiovasc Res* 2000; 48: 265–273.

11 Iriki Y, Ishida S, Oketani N, *et al*. Relationship between clinical outcomes and unintentional pulmonary vein isolation during substrate ablation of atrial fibrillation guided solely by complex fractionated atrial electrogram mapping. *J Cardiol* 2011; 58: 278–286.

12 Altomare C, Terragni B, Brioschi C, *et al*. Heteromeric HCN1-HCN4 channels: a comparison with native pacemaker channels from the rabbit sinoatrial node. *J Physiol* 2003; 549 (Pt 2): 347–359.

13 Tardif JC, Ford I, Tendera M, *et al*. Efficacy of ivabradine, a new selective If inhibitor, compared with atenolol in patients with chronic stable angina. *Eur Heart J* 2005; 26: 2529–2536.

14 Lee MA, Dae MW, Langberg JJ, *et al*. Effects of long-term right ventricular apical pacing on left ventricular perfusion, innervation, function and histology. *J Am Coll Cardiol* 1994; 24: 225–232.

15 Fukuoka S, Nakagawa S, Fukunaga T, *et al*. Effect of long-term atrial-demand ventricular pacing on cardiac sympathetic activity. *Nucl Mad Commun* 2000; 21: 291–297.

16 Scherlag BJ, Patterson E, Po SS. The neural basis of atrial fibrillation. *J Electrocardiol* 2006; 39(4 Suppl): S180–S183.

17 Schauerte P, Scherlag BJ, Patterson E, *et al*. Focal atrial fibrillation: experimental evidence for a pathophysiologic role of the autonomic nervous system. *J Cardiovasc Electrophysiol* 2001; 12: 592–599.

18 Sulfi S, Timmis AD. Ivabradine - the first selective sinus node I(f) channel inhibitor in the treatment of stable angina. *Int J Clin Pract* 2006; 60: 222–228.

19 Borer JS. Drug insight: If inhibitors as specific heart-rate-reducing agents. *Nat Clin Pract Cardiovasc Med* 2004; 1: 103–109.

20 Patterson E, Po SS, Scherlag BJ, *et al*. Triggered firing in pulmonary veins initiated by in vitro autonomic nerve stimulation. *Heart Rhythm* 2005; 2: 624–631.

21 Biel M, Wahl-Schott C, Michalakis S, *et al*. Hyperpolarization-activated cation channels: from genes to function. *Physiol Rev* 2009; 89: 847–885.

22 Wickenden AD, Maher MP, Chaplan SR. HCN pacemaker channels and pain: a drug discovery perspective. *Curr Pharm Des* 2009; 15: 2149–2168.

23 DiFrancesco D, Borer JS. The funny current: cellular basis for the control of heart rate. *Drugs* 2007; 67 (Suppl 2): S15–S24.